SEMI-ANALYTIC MODELING OF SOUND PROPAGATION AND NOISE CROSS-CORRELATIONS IN A COASTAL OCEAN

Oleg A. Godin[a]

[a]Naval Postgraduate School, Monterey, CA, USA

Contact author: Oleg A. Godin, Physics Department, Naval Postgraduate School, 833 Dyer Road, Bldg 232, Monterey, CA 93943, USA. Fax: 831-656-2834. Email: oagodin@nps.edu.

Abstract: *Sound propagation in the coastal ocean over ranges large compared to water depth involves multiple interactions with the ocean surface and bottom. Bathymetric variations and time-dependence of the ocean surface lead to 3-D (such as horizontal refraction) and 4-D (arising from an evolution of the environmental parameters with time) effects being more pronounced in the coastal ocean than in typical deep-water settings. Understanding and modeling sound propagation in horizontally inhomogeneous ocean with time-dependent parameters remains a challenging problem. In this paper, we investigate 3-D and 4-D propagation effects from the prospective of acoustic remote sensing. Analytical techniques are employed to quantify the effects of horizontal refraction on amplitudes and travel times of adiabatic normal modes. Depending on orientation of the propagation path relative to the prevailing seafloor slope, different patterns emerge of the systematic deviation of apparent dispersion curves of adiabatic modes from the dispersion curves in the range-independent waveguide. It is found that, when mode travel times are used as input information for geoacoustic inversions, moderate bottom slopes can lead to large errors in retrieved geoacoustic parameters and cause a positive bias in the bottom sound speed estimates if the horizontal refraction is ignored. In passive acoustic remote sensing, two-point noise cross-correlation functions replace acoustic fields due to a compact controlled sound source as the probing signals which interrogate the environment. Noise averaging times that are necessary to measure two-point cross-correlation functions are much larger than the acoustic propagation times between the two points. As a result, 4-D effects prove to be much stronger in the passive than active remote sensing regime. It will be shown how wind waves and tides limit the usable frequency band of passive acoustic remote sensing in the coastal ocean.*

Keywords: *range-dependent waveguides, horizontal refraction, noise interferometry*

INTRODUCTION

This brief paper provides a sample of the material to be discussed in the conference presentation. Section 2 illustrates the effects of the waveguide range dependence and horizontal refraction of sound on normal mode dispersion, manifestations of these effects when time-warping [1] is applied to isolate modal components of the acoustic field, and their implications for geoacoustic inversions. Section 3 gives an example of the distortions of the empirical Green's function retrieved from noise cross-correlations in a coastal ocean due to motion of the ocean surface during noise averaging.

DISPERSION OF ADIABATIC NORMAL MODES IN A COASTAL WEDGE

Consider guided sound propagation in a homogeneous fluid layer with boundaries, the normal impedances of which depend only on the angle of incidence of a plane wave but not on wave frequency. Examples of such boundaries include pressure-release and rigid surfaces as well as interfaces with homogeneous fluid or solid half-spaces. It is easy to see that, when written in terms of phase speed of normal modes, dispersion equation of such a waveguide contains frequency ω only in the combination ωH, where H is thickness of the fluid layer.

Let sound propagate in a coastal wedge with a strait coastline. Horizontal coordinates x and y are perpendicular and parallel to the coastline, respectively. Water depth $H(x)$ increases linearly with increasing x. In the adiabatic approximation [2], travel time of n-th normal mode is

$$T_n = \int \frac{dx}{u_n} = \cot\alpha \int_{H_1}^{H_2} \frac{dH}{u_n(\omega, H)}. \tag{1}$$

Here H_1 and H_2 are the water depths at the source and receiver locations, $H_1 < H_2$; α is the angle that the seafloor makes with the horizontal plane; and $u_n(\omega, H)$ is the group speed of the local normal mode.

When sound speed in water is constant, phase and group speeds c_n and u_n are functions of ωH in an ideal wedge with pressure-release and/or rigid boundaries and in a penetrable wedge with a pressure-release surface and homogeneous fluid or solid bottom. Then,

$$\frac{1}{u_n} = \frac{1}{c_n} + \omega\left(\frac{\partial}{\partial\omega}\frac{1}{c_n}\right)_H = \frac{1}{c_n} + \omega H \frac{d}{d(\omega H)}\frac{1}{c_n} = \frac{1}{c_n} + H\left(\frac{\partial}{\partial H}\frac{1}{c_n}\right)_\omega = \left(\frac{\partial}{\partial H}\frac{H}{c_n}\right)_\omega. \tag{2}$$

Substitution of the right-most side in Eq. (2) into Eq. (1) gives a closed-form expression for the mode travel time:

$$T_n = \left[\frac{H_2}{c_n(\omega, H_2)} - \frac{H_1}{c_n(\omega, H_1)}\right]\cot\alpha. \tag{3}$$

It is straightforward to extend this result to a more complicated bathymetry, where water depth is piece-wise linear function of x. Then, mode travel time is given by the sum of

contributions Eq. (3) in each segment with a constant bottom slope, the slope α being different in each segment.

In the more general case, when sound propagates at an angle to the seafloor slope,

$$T_n = \int \frac{dl}{u_n} = \int \frac{\sqrt{k_x^2 + k_y^2}}{k_x} \frac{dx}{u_n} = \omega \cot\alpha \int \frac{dH}{u_n \sqrt{\omega^2 - c_n^2 k_y^2}}. \quad (4)$$

Here l stands for arc length along a horizontal (modal) ray; k_x and k_y are the x and y components of the mode's wave vector, and k_y =const. on the horizontal ray. The integral in Eq. (4) is readily evaluated in a closed form in the ideal wedge but numerical integration is needed in the case of the penetrable wedge.

Figure 1 illustrates dependence of mode travel time on frequency at upslope/downslope sound propagation in the penetrable wedge. The most apparent difference between the dispersion curves in the wedge and the Pekeris waveguide with the same average depth is the disappearance (for modes n = 2, 3, 4) or contraction (for mode 1) of the anomalous dispersion part of the curves. In addition, at normal dispersion, instantaneous frequencies tend to be higher, at a given travel time, in the wedge. Another important difference from the range-independent case is the large decrease in the maximum travel time. This can be attributed to the minimum group speed occurring at different frequencies at different depths, so that at all frequencies only a small portion of the entire up- or downslope propagation path is covered at near-minimum group speeds. In the warped domain, contraction of the frequency range or complete disappearance of the anomalous dispersion gives the warping results in the penetrable wedge a much closer resemblance to the results in the range-independent ideal waveguide, where the warped dispersion curves are horizontal lines, than in the case of the Pekeris waveguide.

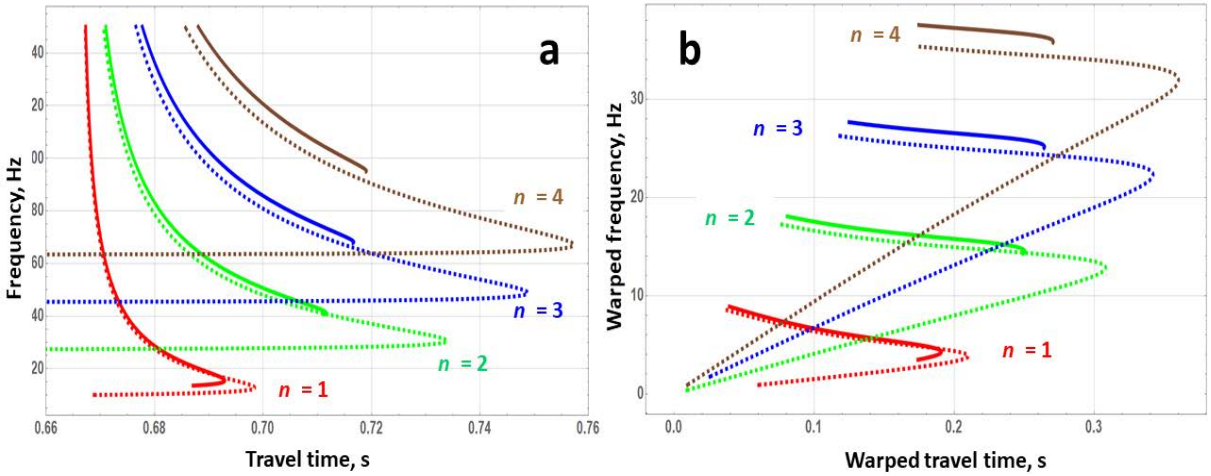

Fig.1: Dispersion curves of the first four adiabatic normal modes in the physical (a) and warped (b) domains at upslope or downslope propagation in a penetrable wedge with a fluid bottom. Source and receiver depths are 50 m and 100 m. Sound speeds in the water column and bottom are c =1500 m/s and c_b =1800 m/s, respectively; the ratio of bottom and water densities m = 2.2. Dashed lines show dispersion curves of normal modes in a range-independent, 75 m-deep waveguide with the same water and bottom parameters and at the same propagation range of 999.167 m.

Figure 2 illustrates modal dispersion at cross-range propagation. Normal modes in a wedge experience stronger dispersion than at propagation over the same range in the Pekeris waveguide with the same physical parameters. This leads to an increase of the received signal duration. In particular, for a fixed frequency range in the normal dispersion band, the

maximum travel time is greatly increased compared to the Pekeris waveguide. Lower frequencies are responsible for later arrivals and are more sensitive to the seafloor slope. In contrast, travel times at higher frequencies, where the value of the group speed approaches the sound speed in water, are insensitive to the slope. The adiabatic mode's travel time reaches its maximum at a higher frequency at cross-slope propagation than in the Pekeris waveguide. At all frequencies considered, sound propagates slower in the wedge than in the Pekeris waveguide. This should be contrasted with the Fermat's principle-related *decrease* in the mode's eikonal (phase) due to horizontal refraction [3].

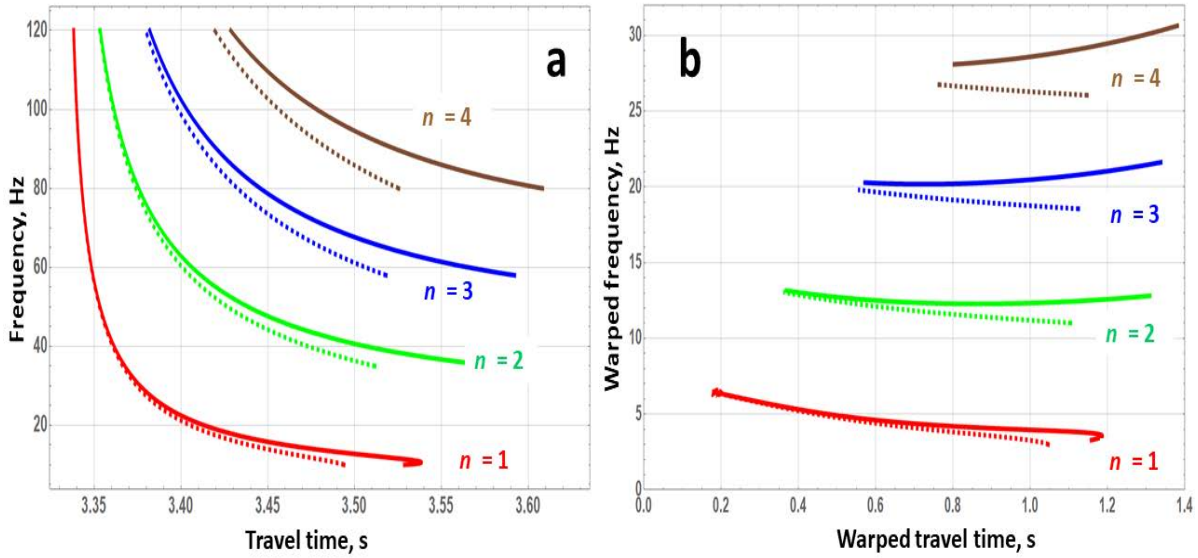

Fig.2: Same as in Fig. 1 but at cross-slope propagation. Source and receiver depths are 100 m. Dashed lines show dispersion curves of normal modes in a range-independent Pekeris waveguide with the same water and bottom parameters and depth of 75 m, at the same propagation range of 5000 m. The dispersion curves are shown in the frequency bands 10–120, 35–120, 58–120, and 80–120 Hz for modes 1, 2, 3, and 4, respectively.

LONR-RANGE NOISE CORRELATIONS AND LOSS OF COHERENCE IN NONSTATIONARY OCEAN

The ocean is a dynamic environment, physical parameters of which evolve in time. In acoustics, the ocean can be often treated as a "frozen" medium with time-independent parameters as long as no appreciable changes occur during the *sound travel time*. This is not the case in acoustic noise interferometry, where the "frozen" medium approximation is justified only when no appreciable changes occur during the much larger *noise averaging time* that is necessary for emergence of an approximation to the deterministic Green's function from cross-correlation functions of diffuse noise. Time-dependence of environmental parameters leads to a deterioration of the long-range correlations of diffuse noise, which underlie the noise interferometry and its applications to passive ocean remote sensing.

Under rather general assumptions, the problem of quantifying the loss of noise coherence in a dynamic ocean proves to be mathematically equivalent to calculating the mean field due to a deterministic point source in an inhomogeneous medium with either random or periodic in time parameters [4]. Figure 3 illustrates coherence loss in a coastal ocean, which is modelled as a Pekeris waveguide, in the presence of tides. To a good accuracy, tides change the water depth simultaneously along the entire sound propagation path between the two receivers involved in evaluation of the noise cross-correlations. A loss of coherence occurs

primarily because the normal mode phase advance at propagation between the receivers changes with the water depth. The coherence loss of individual normal mode components of

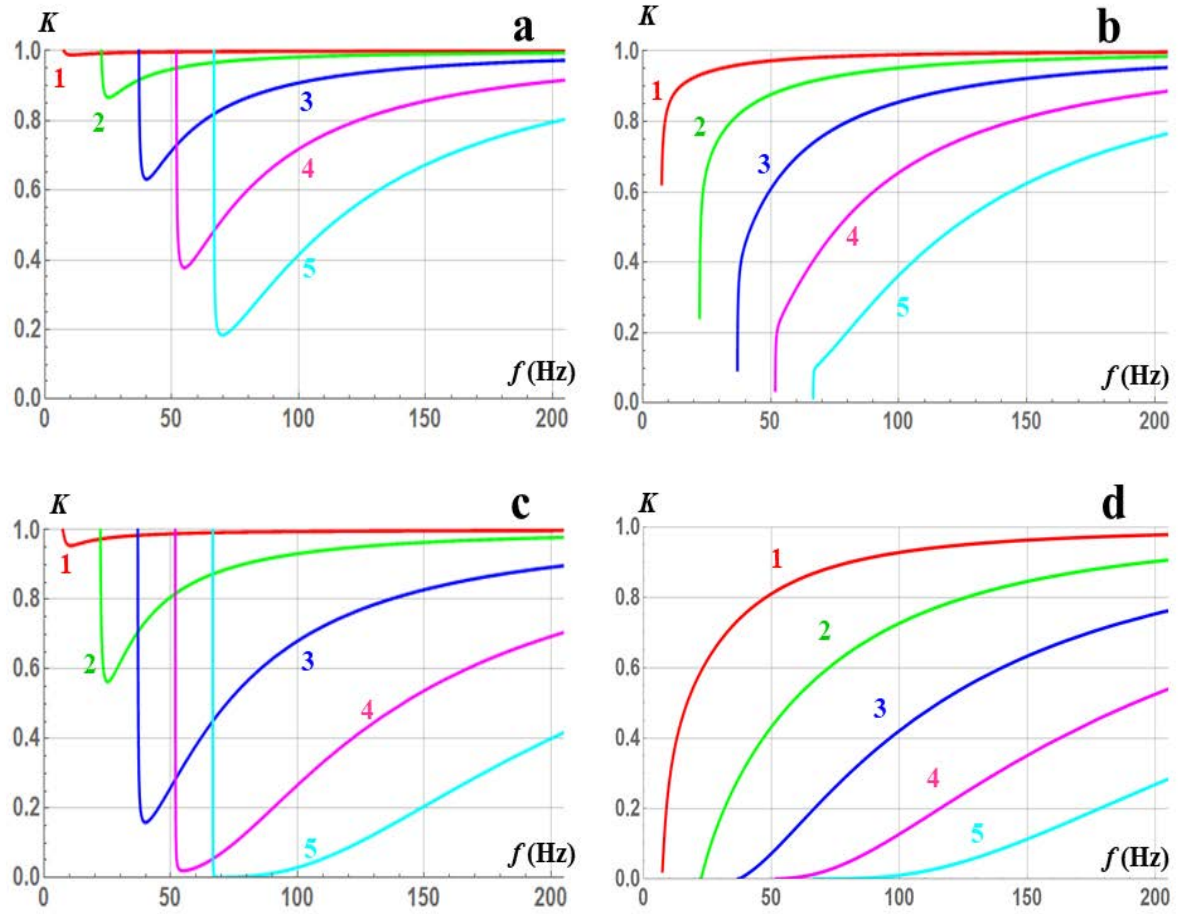

Fig.3: Loss of coherence of normal mode components of noise cross-correlations in a Pekeris waveguide due to ocean surface motion and sound attenuation in the ocean bottom. (a), (c) Coherence loss due to ocean surface motion alone with sound attenuation being negligible. (b), (d) Combined effect of bottom attenuation and surface motion. Horizontal separation of hydrophones is 5 km in panels (a), (b), and 10 km in panels (c), (d). Tidal changes of water depth are modeled as a Gaussian random process with RMS elevation of 0.5 m. Water depth is 100 m; sound speeds in water and fluid bottom are 1537.4 m/s and 1800 m/s; the ratio of bottom and water densities is 2.2. Sound attenuation in the bottom is 0.2 dB/wavelength in panels (b) and (d). Each curve is marked by the order n = 1, 2, 3, 4, 5 of the respective normal mode.

the two-point noise cross-correlation function rapidly increases with range (Figs. 3a, c) similar to the coherence loss of individual surface-reflected rays with a fixed angle of incidence [4]. The trend of the coherence loss to increase with mode order in Fig. 3 is analogous to the increase in coherence loss with angle of incidence of surface-reflected ray arrivals. However, frequency dependence of the coherence loss proves to be rather different for rays and normal modes. For normal modes, the frequency dependence is distinctly non-monotone when absorption is negligible, with zero coherence loss at the cutoff frequency and in the high-frequency limit and a pronounced maximum of the coherence loss at frequencies slightly above the cutoff. This peculiar frequency dependence can be traced back to the fact that the sensitivity of the mode phase to surface elevations is controlled by the derivative of the mode wavenumber, ω/c_n, with respect to water depth H, and

$$\left(\frac{\partial}{\partial H}\frac{\omega}{c_n}\right)_{\omega} = \omega\left(\frac{\partial}{\partial H}\frac{1}{c_n}\right)_{\omega} = \frac{\omega^2}{H}\left(\frac{\partial}{\partial \omega}\frac{1}{c_n}\right)_{H} = \frac{\omega}{H}\left(\frac{1}{u_n} - \frac{1}{c_n}\right). \quad (5)$$

The right-most side of Eq. (5) is zero at mode cutoff and in the high-frequency limit.

Sound absorption in the bottom adds to the coherence loss (Fig. 3b, c) due to exponential decay with range of normal mode amplitudes in the empirical Green's function retrieved from noise cross-correlations. In the Pekeris waveguide, normal mode penetration into the bottom is largest at cutoff and steadily decreases with frequency; at a given frequency, bottom penetration increases with the normal mode order. These properties of normal modes are reflected in the dependencies of the coherence loss on sound frequency and mode order. Note the sharp contrast between frequency dependencies near the mode cutoff of the coherence loss with (Fig. 3b, d) and without (Fig. 3a, c) account for the absorption. In a more realistic scenario, where the bottom attenuation and ocean surface nonstationarity are present simultaneously, the two mechanisms of coherence loss combine and, for the waveguide parameters and the hydrophone separation considered, result in the coherence losses that steadily decrease with frequency and increase with mode order n. Comparison of Figs. 3a–d shows that relative significance of the two mechanisms varies depending on ω an n. However, the relative significance of tides vs. bottom attenuation always increases with increasing horizontal separation of hydrophones.

ACKNOWLEDGEMENTS

This work was supported by the National Science Foundation, grant OCE1657430, and the Office of Naval Research, awards N00014-18-WX-01725 and N00014-19-WX-00462.

REFERENCES

[1] **J. Bonnel and N. R. Chapman**, Geoacoustic inversion in a dispersive waveguide using warping operators, *J. Acoust. Soc. Am.*, 130 (2), pp. EL101–EL107, 2011.

[2] **L. M. Brekhovskikh, and O. A. Godin,** *Acoustics of Layered Media. 2 Point Sources and Bounded Beams*, 2nd edn., Springer, pp. 243–319, 1998.

[3] **O. A. Godin**, A 2-D description of sound propagation in a horizontally-inhomogeneous ocean, *J. Comput. Acoust.*, 10 (1), pp. 123–151, 2002.

[4] **O. A. Godin**, Acoustic noise interferometry in a time-dependent coastal ocean, *J. Acoust. Soc. Am.*, 143 (2), pp. 595–604, 2018.